Forest fire monitoring of Shoolpaneshwar Wildlife Sanctuary, Gujarat, India using geospatial techniques

Shrey Rakholia[1,*], Abhinav Mehta[1] and Bijal Suthar[2]

[1]TGIS, Sarkari Vasahat Road, Vastrapur, Ahmedabad 380 052, India
[2]7/168 Hector Street, Osborne Park, Perth 6017, Australia

Forest fire mapping is essential for monitoring significant ecosystem losses. Geospatial techniques play a considerable role in the monitoring of these events across the globe. The present study observes and compares various indices like NDVI, NBR and RBR used to estimate burn severity, which can be helpful to measure vegetation loss in the study area during 2018. The study shows a strong correlation between NDVI and dNBR, and better differentiation between the burned and unburned regions using RBR to create a better forest action plan for the local state departments to combat forest fires.

Keywords: Burn severity, forest fire, geospatial techniques, vegetation loss, wildlife sanctuary.

FOREST fires cause significant concern in the achievement of climate action goal (Sustainable Development Goal (SDG) 13), as they contribute to increasing carbon dioxide (CO_2) concentration, which further leads to rise in the global temperature. Also, intense forest fires can lead to biodiversity loss as they directly affect the survival of the forest population, which is a concern of SDG 15, i.e. Life on Land[1,2].

Fire regimes are an essential part of the forest ecosystem as they contribute to many ecosystem services, including enhancement of species replacement and pollination, natural pest control, reducing massive catastrophic forest fires, etc.[3]. Studies have shown that almost half the number of protected areas (PAs) in India have been detected with forest fires between 2006 and 2015; during 2014, around 9.4% of the total vegetation in PAs was burnt due to forest fires[4]. This can be attributed to drought conditions as determined by the warming effect of the ocean due to ENSO (El Niño–Southern Oscillation during the Indian monsoon)[5]. Furthermore, the IPCC projections of higher temperatures and worsening drought conditions can aggravate the forest fire severity and frequency, especially in regions like south Gujarat, India, according to the Forest Fire Danger Index (FFDI)[6].

This study analyses forest fires in Shoolpaneshwar Wildlife Sanctuary (SWLS), which is located in the Narmada district, Gujarat, and was notified as a PA in 1982 (ref. 7). The Sanctuary is categorized as tropical savannah (Aw), more precisely equatorial savannah, with dry winter characteristics where minimum precipitation is less than 60 mm in winter[8], as identified by overlaying the Sanctuary area layer on the 'updated Köppen–Geiger climate map of the world' according to Köppen–Geiger climate classification[9].

The SWLS contains nearly around 127 tree species, dominated by teak (*Tectona grandis*) and bamboo (*Dendrocalamus strictus*). Other tree species include mango (*Mangifera indica*), mahua (*Madhuca indica*) and fig (*Ficus glomerata*)[10]. Past studies have shown greater Normalized Difference Vegetation Index (NDVI) values in monsoon attributed to the lush green forest cover conditions. Whereas in summer, the NDVI values were low, attributed to leafless situations. Also, vegetation growth and density were at a peak during monsoon, i.e. the growing season, in contrast to summer (March and April), when greater leaf fall was observed[11].

For monitoring post-fire effects, burn severity mapping is one of the most common approaches used, as it offers timely and cost-effective solutions[12]. The burned areas show higher reflectance in SWIR (shortwave infrared) band and low reflectance in NIR (near infrared) band. As Normalized Burn Ratio (NBR) is the ratio between NIR and SWIR, a positive NBR value indicates unburned (productive) vegetation. In contrast, a negative value suggests burned areas, i.e. those without vegetation, or severe water stress in the vegetation[13,14]. There are alternatives to delta Normalized Burn Ratio (dNBR) such as the relativized burn ratio (RBR), a relativized version of dNBR because the overall classification accuracy of RBR is much more improvized than dNBR[15]. Nevertheless, a high correlation is observed between field-based results and the severity classes yielded using remote sensing techniques, particularly NDVI and differenced Normalised Difference Vegetation Index (dNDVI) (pre-NDVI – post-NDVI), and especially when there is absence of changes in vegetation due to factors such as post-fire rainfall events[16].

The tangible losses, including timber loss due to forest fires in India alone, were estimated at INR Rs 4.4 billion (roughly US$ 100 million) along with direct effects on
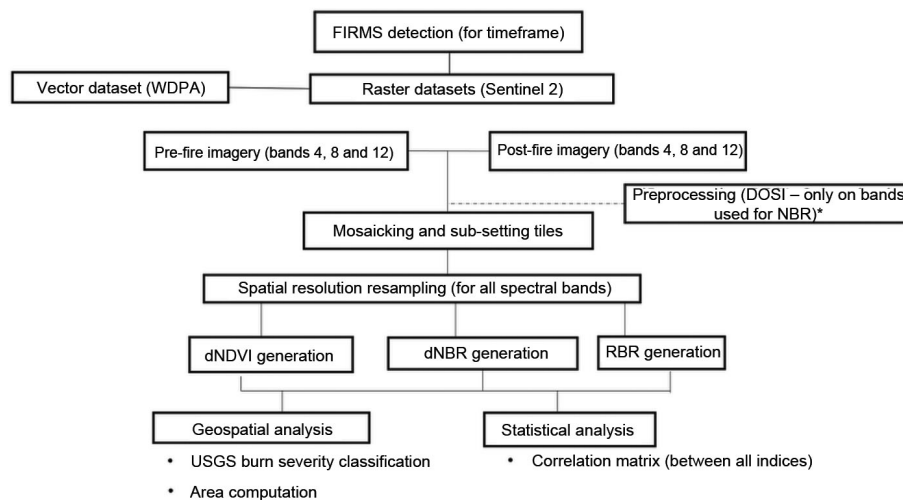
Figure 1. Flowchart showing the methodology used in the present study. *The DOS1 method was only applied to bands used for dNBR and RBR generation.
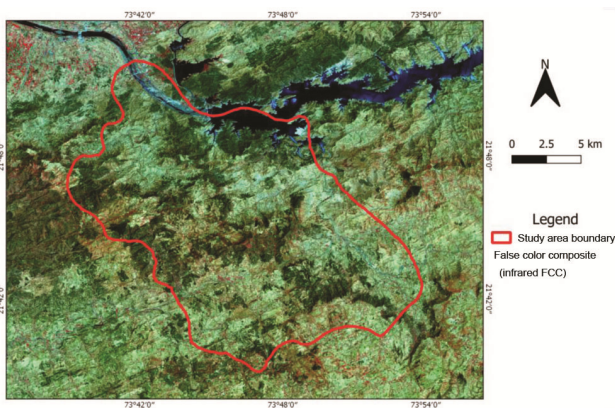

Figure 2. Map showing the study of Shoolpaneshwar Wildlife Sanctuary (SWLS), Gujarat, India.

65 million tribal people whose livelihood depends on non-timber forest products (NTFPs)[17]. The primary objective of this study is to compare three different indices, i.e. NDVI, dNBR and RBR. We expect that this study will help in the effective monitoring of forest fires for the mapping of burned areas in the study area. It aims to provide insights for developing policy and planning in preventing larger forest fire events in future, which would not only help policymakers in the decision-making process, but would also help the local community whose livelihood depends on timber and NTFPs.

Methodology

Figure 1 shows the methodology used in this study.

Study area

The sanctuary consists of semi evergreen moist deciduous forests which are additionally classified into moist teak

forests, dry tropical riverine forests, dry bamboo brakes and shrub forests[18]. The geology of SWLS is mostly hilly, ranging from 400 to 864 m amsl consisting of moderate to steep slopes. The average maximum summer temperature recorded was 43°C and average minimum winter temperature was 8°C. Average mean rainfall of 1000 mm was recorded during June to October in SWLS[19]. The vector dataset of SWLS was obtained from the World Database of Protected Areas (WDPA), which is a part of the protected planet-on-line platform maintained by the UN Environment and the International Union for Conservation of Nature (IUCN). The SWLS falls under IUCN Management Category 4 according to the WDPA, which comprises of a reported area of 607.7 sq. km (ref. 20). However, the vector dataset obtained has an area of 330.8 sq. km according to the WDPA extracted boundary of SWLS, which falls in the geographic extent between 21°38′ and 21°51′N lat, 73°38′ and 73°53′E long (Figure 2).

Datasets and pre-processing

Datasets: The satellite dataset used in this study was obtained from Copernicus Open Access Hub. It contained four level-1 C raster images (tiles) of Sentinel 2, i.e. 2A and 2B satellites with sensing dates on 2 February 2018, for the pre-fire scene and on 8 April 2018, for the post-fire scene (Table 1). These images were provided in top-of-atmosphere (TOA) reflectance obtained from the MSI (multi-spectral instrument) sensors of the satellites. The dataset consists of tiles of area 100×100 sq. km, ortho-rectified in UTM/WGS84 projection and containing 13 different spectral bands[21]. Among the 13 spectral bands, the bands of interest include band 4 (red), band 8 (NIR), and band 12 (SWIR 2). The original spatial resolution

Table 1. Spatial and temporal details of each dataset (satellite imagery) used in the analysis

Dataset (tile position)	Sensing date	Tile no.	Bands used
Pre-fire (north)	2 February 2018	T43QCE	B4, B8, B12
Pre-fire (south)	2 February 2018	T43QCD	B4, B8, B12
Post-fire (north)	8 April 2018	T43QCE	B4, B8, B12
Post-fire (south)	8 April 2018	T43QCD	B4, B8, B12

Table 2. Spectral characteristics and spatial resolution of the Sentinel 2 bands used in this analysis

Spectral band characteristics			Spatial resolution (m)	
Spectral band	Spectral region	Wavelength range (nm)	Before resampling	After resampling
Band 4	Red	650–680	10	20
Band 8	Near-infrared (NIR)	785–900	10	20
Band 12	Shortwave-infrared (SWIR2)	2100–2280	20	20

of the raster datasets for band 4, band 8, and band 12, was 10, 10 and 20 m respectively. Cloud-free satellite images (pre-fire and post-fire images are listed in Table 1) were obtained for the analysis. In this study, we followed the extended assessment strategy, where the pre-fire scene was taken from the same season and year of the fire, whereas the post-fire scene was taken after the fire but before the next growing season. The extended assessment is a better representative of the actual severity than the initial assessment where the pre-fire imagery comes from past years and thus disturbances in the landscape between past year (pre-fire) and current year (post-fire) could affect the estimations[13].

Forest fire detection: The fire was detected by FIRMS (Fire Information for Resource Management System), where several patches in the SWLS were affected between February 2018 and March 2018. FIRMS is an on-line web platform of NASA, USA, that provides fire and hotspot data within which the MODIS Terra/Aqua global burned area product (MCD64A1) provides detection of burns at approximate dates with a spatial resolution of 500 m and spatial coverage of global level[22]. In this analysis, the FIRMS platform was used to detect the extent of forest fires in the SWLS area and the approximate month range for pre-fire and post-fire scenes.

Pre-processing

Satellite images acquired were geo-rectified using geographic projection system in QGIS with WGS84 Datum. The dark object subtraction (DOS) is an image pre-processing technique used to eliminate haze to correct light scattering in satellite data based on the premise that the occurrence of absolute black features on the Earth's surface is rare[23]. In this analysis, we have used DOS1 method in semi-automatic classification plugin (SCP) in QGIS, because the simple correction by this method provides better results as far as using multi-temporal images

are concerned, and thus it is commonly used as an image pre-processing method in change detection analysis[24]. The DOS1 correction method is the most basic of the DOS methods (the others being DOS2, DOS3 and DOS4)[25].

Mosaicing and sub-setting: The requirement of mosaicing in this analysis was to merge the two north (T43QCE) and south (T43QCD) Sentinel-2 satellite tiles for both pre-fire and post-fire images, as the study area falls between those tiles. After mosaicing was done, sub-setting was carried out for the raster images, which were clipped by considering the WDPA boundary. Also, spectral sub-setting was done simply by choosing only the three spectral bands (i.e. bands 4, 8 band 12), which were required for the analysis.

In Table 2, the spectral characteristics are shown, including the spectral region and wavelength range (nm), which basically are of the MSI sensor[26]. We resampled the spatial resolution using QGIS for band 4 (10 m) and band 8 (10 m) to adjust with the resolution of band 12 (20 m). Thus, all three spectral bands were matched to 20 m resolution.

Normalized burn ratio generation

NBR analysis was performed to identify mainly the burned areas and further classify them using satellite images according to USGS burn severity classification. The equation to compute NBR is similar to NDVI, but it uses SWIR2 (2100–2280 nm) reflectance instead of visible (red), which is given by eq. (1).

NBR was computed on both pre-fire and post-fire scene raster images. dNBR is usually calculated by the difference in the image of NBR pre-fire and post-fire scenes, which gives a quantitative measure of the vegetation change due to the fire event, as shown in eq. (2).

$$\text{NBR} = \frac{\text{NIR} - \text{SWIR2}}{\text{NIR} + \text{SWIR2}}, \tag{1}$$

$$dNBR = \text{Pre-fire NBR} - \text{Post-fire NBR}. \tag{2}$$

Once dNBR is computed according to eq. (2), dNBR can be interpreted by considering the negative values as enhanced regrowth or absence of burn in vegetation cover, whereas the positive values can be seen as a set of burned severity values from low to high. One of the widely used classification systems is the USGS burn severity universal threshold with values ranging from –0.5 to +1.3; it was used in this study to interpret dNBR values accurately, as described in the Fire Effects Monitoring and Inventory System (FIREMONS)[13]. The method described by FIREMONS is a classification that includes seven classes based on different dNBR ranges (Table 3).

Normalized difference vegetation index generation

NDVI is computed from the ratio of NIR and red band reflectance as shown in eq. (3), since the red wavelength region is absorbed by chlorophyll present in the vegetation, whereas the mesophyll scatters NIR. NDVI values have a range from –1 to +1, and negative values indicate that the vegetation is mostly absent[27].

$$NDVI = \frac{\text{NIR} - \text{red}}{\text{NIR} + \text{red}}. \tag{3}$$

After NDVI is computed for both the pre-fire and post-fire scenes, dNDVI is calculated simply by the difference between the pre-fire and post-fire NDVI values thus making dNDVI a bi-temporal index (the difference between values of the index pre-fire and post-fire scenes) as shown in eq. (4).

$$dNDVI = \text{Pre-fire NDVI} - \text{Post-fire NDVI}. \tag{4}$$

The traditional field surveys for obtaining field-measured index, e.g. composite burn index (CBI) are old practices for identifying burned areas, but are tedious and expensive. Hence, remote sensing-derived indices such as NDVI when used in comparison with dNBR have proven to be a reasonable alternative[28].

Table 3. Burn severity classification from FIREMONS with delta Normalized Burn Ratio (dNBR) ranges for severity classes[13]

Severity level	dNBR value range
Enhanced regrowth, high (post-fire)	–0.500 to –0.251
Enhanced regrowth, low (post-fire)	–0.250 to –0.101
Unburned	–0.100 to +0.099
Low severity	+0.100 to +0.269
Moderate–low severity	+0.270 to +0.439
Moderate–high severity	+0.440 to +0.639
High severity	+0.640 to +1.300

Relativized burn ratio generation

RBR is a relativized metric of dNBR, i.e. it is an indicator of change that is relative to the pre-fire vegetation cover conditions, which would theoretically mean that it is more suitable for burn severity at a relative localized scale in comparison to dNBR. As shown in eq. (5), RBR is computed by dividing dNBR by pre-fire NBR values plus 1.001. The reason 1.001 is added to the denominator is to make sure that it will prevent rendering an infinity output as by making sure that the denominator avoids getting a zero value[15].

$$RBR = \frac{dNBR}{\text{Pre-fire NBR} + 1.001}. \tag{5}$$

Correlation matrix generation between indices

In order to determine how much correlation is present, i.e. correlation coefficient (r value), or if there are linear or nonlinear relationships between these indices, a scatterplot is useful. It is done mainly for comparison of the sensitivity of one index with another based on their values[29]. In this analysis also, we have used the scatterplot matrix for pairwise comparison of the three indices, viz. dNBR, dNDVI and RBR, as well as density plots to compare sensitivity for higher or lower values (in raster pixels) with the respective indices using R statistical software. This was achieved by generating 100 random points in QGIS by stratified random sampling method for all the three raster layers of indices.

Results and discussion

Spatial analysis

First, NDVI maps were computed using Sentinel 2 data for pre-fire and post-fire NDVI values. Figure 3 shows a significant decrease in vegetation cover in the study area as depicted from the pre-fire and post-fire NDVI values due to the fire events.

The overall NDVI analysis of SWLS shows that the northwest, centralwest, and few scattered but concentrated patches in the southwest of the study area have been heavily affected due the fires (Figure 4). We have also assumed that all the negative values of NDVI maps indicate unburned areas, because the water bodies present in the study area represent negative NDVI values. As shown in Figure 4, higher dNDVI values indicate higher forest fire impact in the study area, i.e. reduction in the vegetation cover from pre-fire to post-fire scenes.

While comparing Figures 4 and 5, the areas with higher values of dNDVI are those where the NDVI values have reduced considerably between pre-fire and post-fire, i.e.

where the vegetation cover has decreased. As seen in Figure 5, the dNBR map does not sharply distinguish the high severity areas better; hence the relativized version of dNBR, i.e. RBR was computed in order to provide clear differentiation between the burned and unburned areas. The reason for using any relativized index such as RBR is to increase the mapping accuracy of the burned areas. Figure 6 clearly shows the differentiation between burned areas, i.e. areas with higher RBR value and unburned areas, i.e. areas with lower RBR value. Hence, RBR provides a better correlation with pre-fire scene conditions similar to a field measured index[30].

Based on dNBR analysis and further reclassification using the USGS burn severity classes to produce a burn severity map, we found out using the 'calculate unique values table' tool in QGIS that total 21.36%, i.e. 70.66 sq. km of the total area of SWLS was affected by the February–March 2018 forest fires ranging from low to high burn severity. The DOS correction method was used to avoid misclassification of water bodies in the high burn severity category; instead, it was classified in

the enhanced regrowth category (Figure 7). Otherwise, the misclassification would have rendered a larger area of high burn severity category and it is evident that water bodies cannot undergo high burn severity from forest fires. However, maximum area (67.96%, i.e. 224.82 sq. km) of SWLS remained unburned, which implies that the intensity of forest fire events was low. Also, the area where high enhanced regrowth was observed mainly included water bodies, as explained earlier, which constituted 2.1% (7.12 sq. km) of the total area. Other patches were of low enhanced regrowth, which was 8.5% (35.32 sq. km) of the total area (Table 4).

In a study related to burn severity mapping, it was observed that while mapping dNBR some patches of water bodies were classified in high burn severity category[31]. Thus, overall the study provides a simple solution to avoid classifying water bodies into burn severity categories. Although, areas are classified under high enhanced
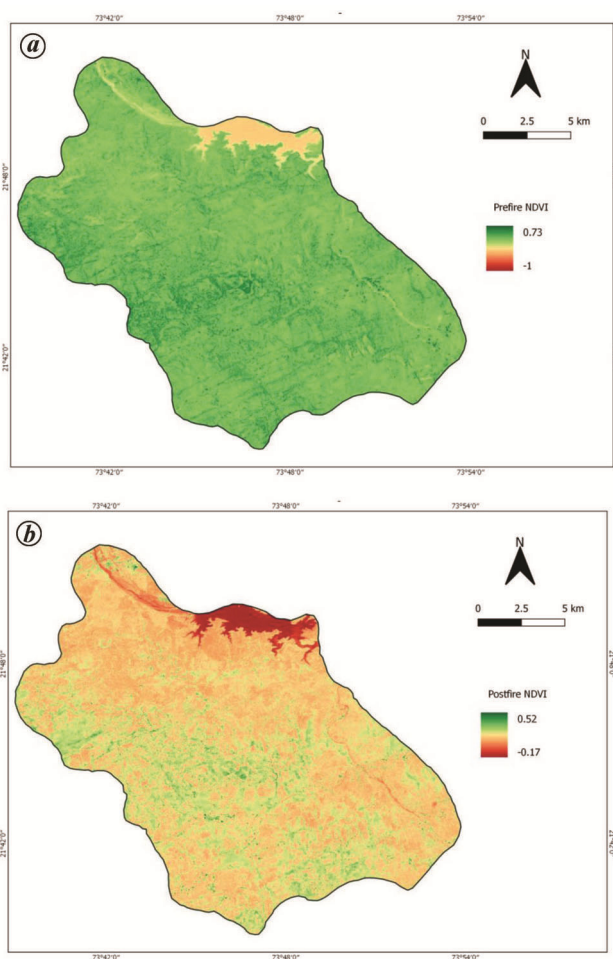

Figure 4. dNDVI (Difference image of pre-fire and post-fire NDVI) map of SWLS.

Figure 3. Normalized difference vegetation index (NDVI) map for (*a*) pre-fire and (*b*) post-fire scene of SWLS.

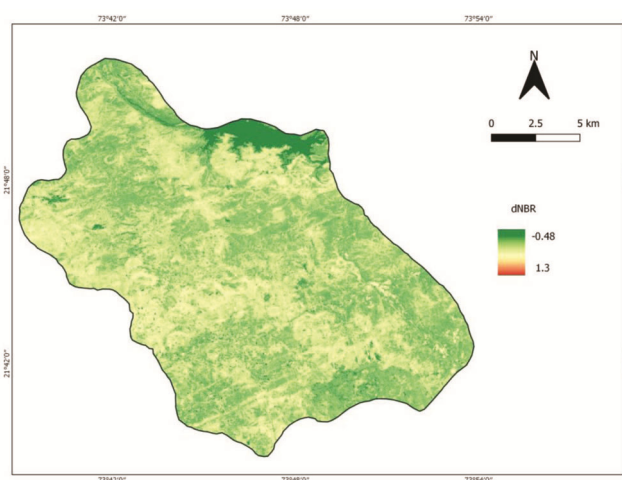**Figure 5.** dNBR (difference image of pre-fire and post-fire Normalized Burn Ratio (NBR)) map of SWLS.

regrowth, it does not significantly affect the burn severity categories area estimation (all categories from unburned to high severity).

Statistical analysis

When statistically evaluating all three indices, we found a strong correlation between dNDVI and dNBR ($r = 0.909$).

Table 4. Area (sq. km.) with the respective burn severity class computed in the analysis

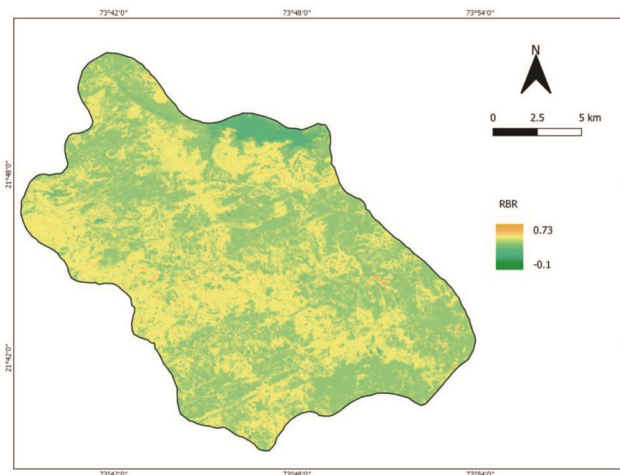| Severity class	Area (sq. km)
High enhanced regrowth	7.12
Low enhanced regrowth	28.19
Unburned	224.82
Low severity	65.32
Moderate–low severity	5.16
Moderate–high severity	0.17
High severity	0.0024
Total	330.80

Figure 6. RBR (relativized version of dNBR) map of SWLS.
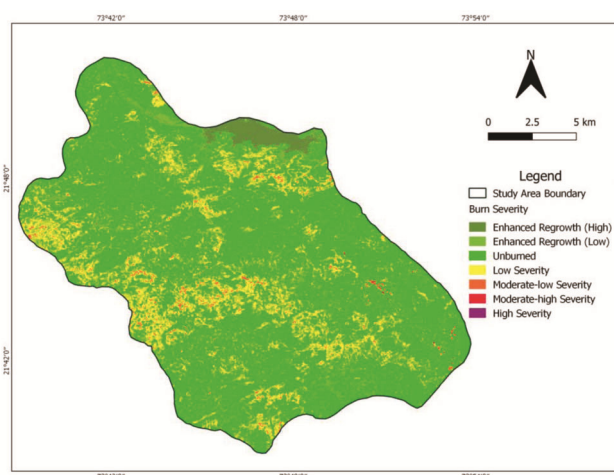

Figure 7. Burn severity map of SWLS based on dNBR.

On the other hand, the correlation between RBR and dNBR was relatively high ($r = 0.979$). However, there was a slightly lower correlation between dNDVI and RBR ($r = 0.847$). Hence, the overall correlation for all three indices, i.e. dNBR, RBR, dNDVI reveals a similar pattern, i.e. highly strong and positive correlation between the indices. Also, a moderate correlation was found in unburned category. We also statistically evaluated the correlation between different categories of dNBR with other indices. More importantly, there was highly strong correlation across all dNBR categories between dNBR and RBR. A robust correlation was observed between classes, viz. high, moderate–high severity, and enhanced regrowth of dNBR and dNDVI for which low and high enhanced regrowth categories were merged together for ease. However, there was a weak correlation observed in categories like low and moderate–low severity. Similar *r* values have been observed between dNBR and dNDVI as well as between dNDVI and RBR for enhanced regrowth ($r \approx 0.9$), unburned ($r \approx 0.4$) and low severity ($r \approx 0.3$) categories. Also, enhanced regrowth and low severity categories have a strong and weak correlation respectively, between dNDVI and the other two indices (Figure 8).

Even though dNBR has universal threshold values provided by USGS, there is a strong positive correlation with dNDVI in this study. Moreover, areas with enhanced regrowth, moderate–high, and high burn severity categories have a strong correlation between dNDVI and dNBR, and therefore can be used together to map burned areas, especially of high burn severity. However, in case of other climatic conditions and forest types, RBR can be a better representative of overall burn severity if a strong correlation across all classes is observed between RBR and dNDVI.

Conclusion

As there is a strong correlation between NDVI and dNBR, we conclude that if these indices are used together, it can give a better estimation of impacted areas due to forest fires and the burn severity together. In addition, RBR also serves as an essential indicator for better differentiation between burned and unburned areas in localized conditions. Due to funding limitations, the ground truth survey was not possible during the study period; it would have provided better validation of the burned areas. However, as there are limitations of mapping based on satellite data, especially in terms of spatial resolution, we recommend the use of aerial (drone), multi-spectral sensors for forest fire surveys in any particular region for more accuracy in burn severity mapping. Also, it would become easier to estimate the loss of forest products in the Sanctuary and nearby areas. The local community depends on these products for its livelihood and thus it
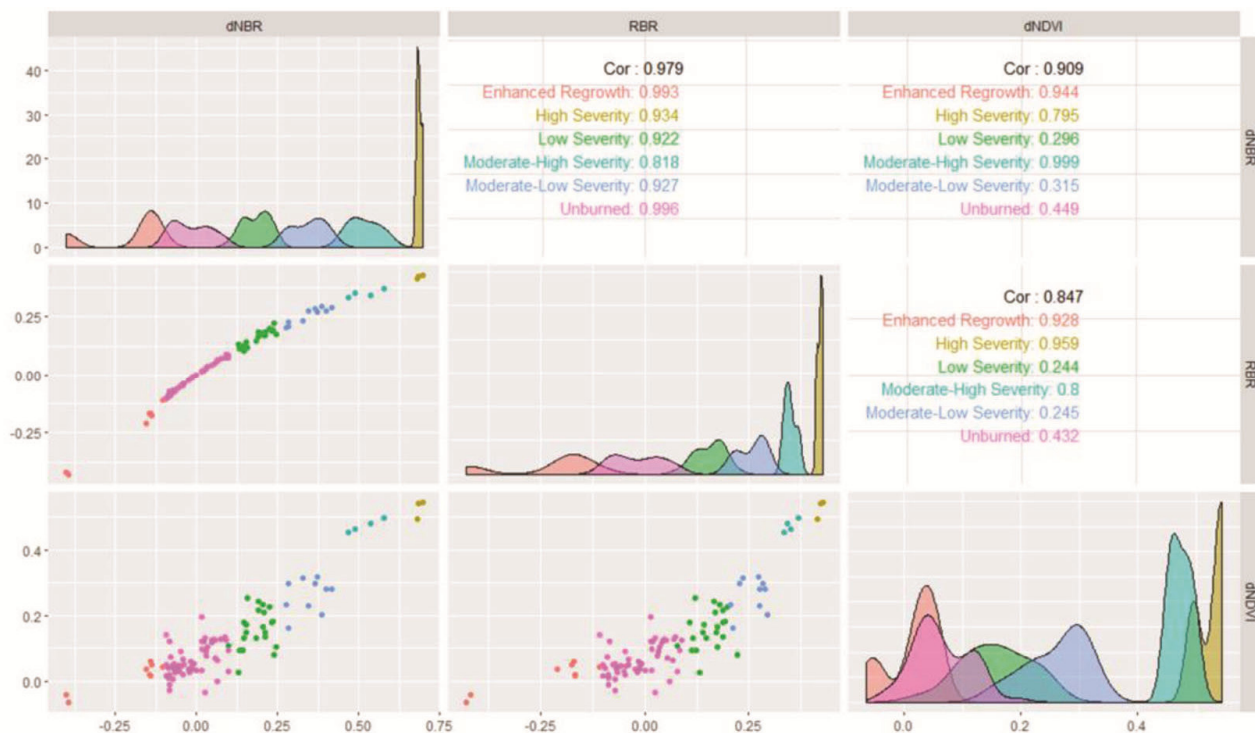
Figure 8. Scatterplots and density plots showing the distribution of random points categorized by dNBR classes. The correlation coefficient (*r* value) between the three indices is also shown.

would be helpful to create a working and management action plan for the near future.

1. Gill, A. M., Stephens, S. L. and Cary, G. J., The worldwide 'wild-fire' problem. *Ecol. Appl.*, 2013, **23**, 438–454.
2. UN Environment Program, The effect of wildfires on sustainable development, 2020; https://www.unenvironment.org/news-and-stories/story/effect-wildfires-sustainable-development (accessed on 20 May 2020).
3. Pausas, J. G. and Keeley, J. E., Wildfires as an ecosystem service. *Front. Ecol. Environ.*, 2019, **17**, 289–295.
4. Reddy, C. S. *et al.*, Monitoring of fire incidences in vegetation types and protected areas of India: implications on carbon emissions. *J. Earth Syst. Sci.*, 2017, **126**(1), 11.
5. Kumar, K. K., Rajagopalan, B., Hoerling, M., Bates, G. and Cane, M., Unraveling the mystery of Indian monsoon failure during El Niño. *Science*, 2006, **314**, 115–119.
6. Settele, J. *et al.*, Terrestrial and inland water systems. In Climate Change 2014: Impacts, Adaptation and Vulnerability: Part A. Global and Sectoral Aspects, Cambridge University Press, 2015, pp. 271–360.
7. Gujarat State Forest Department, Gujarat Forest Statistics 2016–2017, Vadodara, 2017.
8. Kottek, M., Grieser, J., Beck, C., Rudolf, B. and Rubel, F., World map of the Köppen–Geiger climate classification updated. *Meteorol. Z.*, 2006, **15**, 259–263.
9. Peel, M. C., Finlayson, B. L. and McMahon, T. A., Updated world map of the Köppen–Geiger climate classification. *Hydrol. Earth Syst. Sci.*, 2007, **11**, 1633–1644.
10. Christian, B. and Krishnayya, N. S. R., Classification of tropical trees growing in a sanctuary using Hyperion (EO-1) and SAM algorithm. *Curr. Sci.*, 2009, **96**, 1601–1607.
11. Christian, B. *et al.*, Seasonal variations in phenology and productivity of a tropical dry deciduous forest from MODIS and hyperion. *Agric. For. Meteorol.*, 2015, **214–215**, 91–105.
12. Chu, T. and Guo, X., Remote sensing techniques in monitoring post-fire effects and patterns of forest recovery in boreal forest regions: a review. *Remote Sensing*, 2013, **6**, 470–520.
13. Lutes, D. C. *et al.*, FIREMON: fire effects monitoring and inventory system. General Technical Report, USDA Forest Service RMRS-GTR-164-CD, 2006, pp. 1–55.
14. Key, C. H. and Benson, N., Measuring and remote sensing of burn severity. In Proceedings Joint Fire Science Conference and Workshop (ed. Neuenschwander, L. F.), University of Idaho and International Association of Wildland Fire, Moscow, ID, 1999, p. 284.
15. Parks, S. A., Dillon, G. K. and Miller, C., A new metric for quantifying burn severity: the relativized burn ratio. *Remote Sensing*, 2014, **6**, 1827–1844.
16. Chafer, C. J., Noonan, M. and Macnaught, E., The post-fire measurement of fire severity and intensity in the Christmas 2001 Sydney wildfires. *Int. J. Wildl. Fire*, 2004, **13**, 227.
17. Sivakumar, M. V. K., Roy, P. S., Harmsen, K. and Saha, S., Forest fire and degradation assessment using satellite remote sensing and geographic information system. *Satellite Remote Sensing GIS Appl. Agric. Meteorol.*, 2004, **235**, 361–400.
18. Vyas, R., Reptilian diversity in and around the Shoolpaneshwar Wildlife Sanctuary, Gujarat, India. *Reptile Rap.*, 2011, **11**, 5–15.
19. Gupta, R. and Sharma, L. K., Efficacy of spatial land change modeler as a forecasting indicator for anthropogenic change dynamics over five decades: a case study of Shoolpaneshwar Wildlife Sanctuary, Gujarat, India. *Ecol. Indic.*, 2020, **112**, 106–171.
20. Protected Planet, Shoolpaneswar (Dhumkhal) in India; https://www.protectedplanet.net/9241

21. Sentinel ESA, Data Products; https://sentinel.esa.int/web/sentinel/missions/sentinel-2/data-products

22. Fire Information for Resource Management System, Fire map, https://firms.modaps.eosdis.nasa.gov/map/

23. Chavez, P. S., An improved dark-object subtraction technique for atmospheric scattering correction of multispectral data. *Remote Sensing Environ.*, 1988, **24**, 459–479.

24. Song, C., Woodcock, C. E., Seto, K. C., Lenney, M. P. and Macomber, S. A., Classification and change detection using landsat TM data. *Remote Sensing Environ.*, 2001, **75**, 230–244.

25. Congedo, L., Semi-automatic classification plugin documentation release 4.8.0.1. *Release*, 2016, **4**, 29.

26. Hawryło, P. and Wezyk, P., Predicting growing stock volume of scots pine stands using Sentinel-2 satellite imagery and airborne image-derived point clouds. *Forests*, 2018, **9**(5), 274.

27. Pettorelli, N., Vik, J. O., Mysterud, A., Gaillard, J. M., Tucker, C. J. and Stenseth, N. C., Using the satellite-derived NDVI to assess ecological responses to environmental change. *Trends Ecol. Evol.*, 2005, **20**, 503–510.

28. Teodoro, A. and Amaral, A., A statistical and spatial analysis of portuguese forest fires in summer 2016 considering landsat 8 and sentinel 2A data. *Environments*, 2019, **6**(3), 36.

29. Wang, F., Huang, J. and Chen, L., Development of a vegetation index for estimation of leaf area index based on simulation modeling. *J. Plant Nutr.*, 2010, **33**, 328–338.

30. Miller, J. D. and Thode, A. E., Quantifying burn severity in a heterogeneous landscape with a relative version of the delta normalized burn ratio (dNBR). *Remote Sensing Environ.*, 2007, **109**, 66–80.

31. Philipp, M. B. and Levick, S. R., Exploring the potential of C-band SAR in contributing to burn severity mapping in tropical savanna. *Remote Sensing*, 2020, **12**, 49.